Synthesis of single-walled carbon nanotubes under conditions of double spatial confinement in a Si−SiC system

© S.Iu. Priobrazhenskii[1,2], M.G. Mynbaeva[1], E.V. Gushchina[1], A.N. Smirnov[1], D.G. Amelchuk[1], V.Yu. Davydov[1], A.A. Lebedev[1]

[1] Ioffe Institute,
194021 St. Petersburg, Russia
[2] St. Petersburg Electrotechnical University „LETI"
197022 St. Petersburg, Russia

E-mail: sergei.prioby@mail.ioffe.ru

Received May 5, 2026
Revised July 7, 2026
Accepted July 8, 2026

A new catalyst-free method for synthesizing single-walled carbon nanotubes under conditions of double spatial confinement is presented. The method is based on the use of a silicon carbide sandwich structure with a fixed submicron gap. This configuration enables the growth of single-walled carbon nanotubes via „vapor−liquid−solid" mechanism inside microdroplets formed in the gap during the condensation of silicon vapor.

Keywords: silicon carbide, carbon nanotubes, sandwich structure, catalyst-free synthesis.

DOI: 10.61011/SC.2026.05.63991.9636

1. Introduction

The need to develop catalyst-free methods for synthesizing carbon nanotubes (CNTs) stems from the demand for pure structures and CNT-based materials for emerging technologies in nanoelectronics and nanosensing [1–5]. Currently, CNTs are predominantly produced by catalytic methods based on chemical vapor deposition and subsequent decomposition of hydrocarbons on metallic catalysts, namely transition-metal nanoparticles. Residual metallic impurities are a significant problem that requires additional purification of the resulting nanostructures [5,6].

This work discusses a catalyst-free method for producing ordered arrays of single-walled carbon nanotubes (SWCNTs) under double spatial confinement in the submicron gap of a silicon carbide (SiC) sandwich structure. Silicon (Si) melt microdroplets formed in the gap served as microreactors in which nanoscale substructures grew through the „vapor–liquid–solid" (VLS) mechanism. Understanding nanostructure formation under spatial confinement is an important objective of modern materials science [7].

2. Experimental methods

The sandwich structures consisted of two plane-parallel silicon carbide wafers of the hexagonal polytypes 4*H*-SiC and 6*H*-SiC. The gap between the wafers was precisely set by the height of atomic steps (~ 10 nm) produced on their surfaces by preliminary vacuum annealing. Vapor was supplied to the gap from an external solid source (single-crystal silicon) by thermal evaporation under radio frequency (RF) heating in vacuum (1500−1600 °C). After the experiments the wafers were separated. Their surfaces were examined using scanning probe microscopy (SPM) and micro-Raman spectroscopy (μ-RS).

3. Experimental results and discussion

All SPM measurements were performed with an NTegraAura microscope (NT-MDT, Russia) in semicontact mode using HA_FM probes (TipsNano, Russia). The results revealed microstructures on the SiC wafer surfaces with diameters of $\sim 10\,\mu$m, located mainly along crystallographic steps (Figure 1). The representative SPM image of the 4*H*-SiC wafer surface shows that the microstructures contain two types of substructures: dense vertical bundles in the center and a peripheral rim of microcrystallites forming discontinuous ring-shaped substructures.

The SPM images and corresponding profiles in Figure 2 show that the vertical substructures reach 120−180 nm in height, whereas the ring-shaped structures are 20−50 nm high.

The μ-RS spectra were measured in backscattering geometry at room temperature using a LabRAM HREvo UV-VIS-NIR-Open spectrometer (Horiba, France) with a confocal microscope. An Nd:YAG laser at 532 nm provided excitation. The laser beam was focused onto the sample to a spot diameter of $\sim 1\,\mu$m using a 100× Olympus objective with NA = 0.9.

Figure 3 shows a μ-RS spectrum measured in the region of a bundle of vertical substructures. It contains bands peaking at $\sim 1597\,\mathrm{cm}^{-1}$ (G mode) and $1354\,\mathrm{cm}^{-1}$ (D mode), as well as their overtones ($2G$ and $2D$) at 2926 and $2696\,\mathrm{cm}^{-1}$, respectively. These lines are the principal characteristic modes of carbon structures (graphene, CNTs, etc.). The G band corresponds to vibrations of

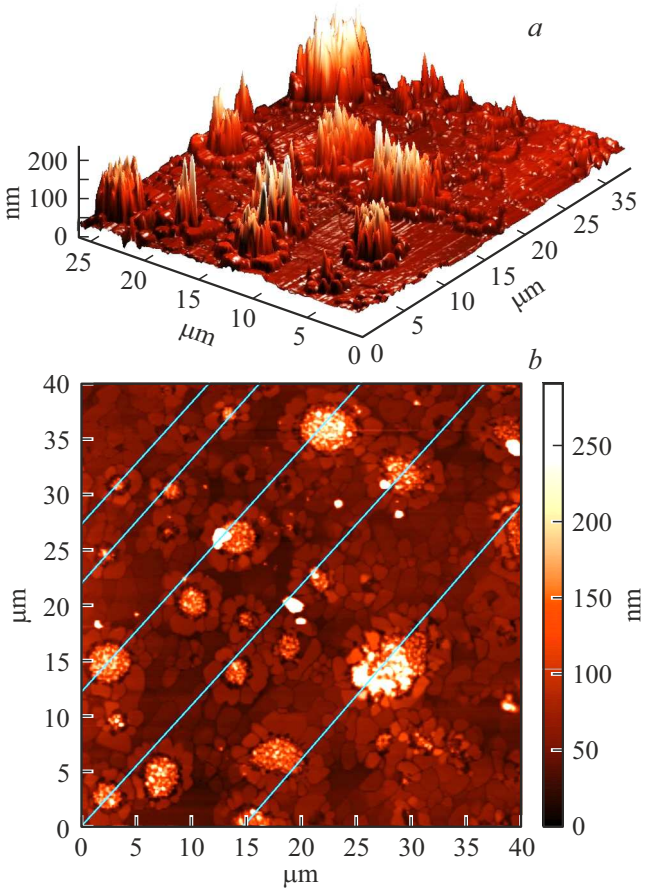


Figure 1. SPM topography of a 4*H*-SiC wafer surface. *a* — 3D view of the surface microstructures; *b* — image showing the distribution of microstructures along crystallographic steps (solid lines).

sp^2-hybridized carbon bonds. The *D* band is associated with structural disorder.

In addition to the main bands characteristic of carbon structures, lines at $\omega_1 = 154\,\text{cm}^{-1}$ and $\omega_2 = 281\,\text{cm}^{-1}$ were detected in the low-frequency part of the μ-RS spectra (see the inset in Figure 3). These lines can be assigned to radial breathing modes (RBMs) [8], which are a distinctive signature of single-walled carbon nanotubes. Thus, the vertical substructures investigated here can be identified as SWCNTs. Nanotube diameters can be determined from the RBM positions. Our calculations based on Ref. [8] show that the vertical substructures contain SWCNTs with diameters of 0.86 and 2.2 nm, corresponding to 281 and $154\,\text{cm}^{-1}$.

The μ-RS spectra of the ring-shaped substructures and the substrate regions between them correspond to crystalline 4*H*-SiC. No additional carbon phases were detected in these regions.

Based on these results, we suggest that the complex microstructures form through processes at the three-phase boundary and within discrete droplets of condensed Si vapor, following the „vapor–liquid–solid“ mechanism. Technologies based on VLS processes are widely used to fabricate nanostructures from $A^{III}B^{V}$ materials. In particular, VLS growth methods are known for structures with similar topologies, such as nanowires and nanorings [9]. Nanostructures are formed by vapor deposition of carbon precursors onto metallic catalyst droplets that do not react chemically with the substrates. A distinctive feature of the Si–SiC system considered here is that the liquid Si phase and SiC substrates react under similar experimental conditions [10].

On the basis of known VLS mechanisms, we propose a simplified scheme for CNT growth in the sandwich-structure gap containing liquid silicon microdroplets.

3.1. Formation of silicon microdroplets

Restricted vapor escape from the submicron gap of the SiC sandwich structure leads to a high Si atom concentration. Monoatomic steps on the SiC surface act as energetically favorable adsorption sites for vapor-phase adatoms. During annealing above the Si melting point, adatoms diffusing along the steps condense into liquid-phase microdroplets (Si melt).

3.2. Formation of the crystalline rim around CNT bundles

As SiC reacts with the Si melt, carbon is transferred from the solid phase into the melt until its solubility limit is reached. Microconvection (Marangoni convection) at the three-phase contact line ($Si_{vap}–Si_{liq}–SiC_{sol}$) raises the carbon concentration above its value in the droplet bulk. Under these conditions, the phase boundary becomes a site for heterogeneous nucleation of SiC microcrystals, which form a ring-shaped structure (see Figure 2). The inner diameter of the rings can be assumed to be determined by the diameter of the condensed liquid droplets.

3.3. Formation of CNT bundles in the microstructure center

Conditions beneath a melt droplet differ fundamentally from those at its periphery. Carbon nanotubes form through „secondary crystallization“ of carbon atoms released from the substrate, creating a locally supersaturated region at the melt–substrate interface. Since no pure silicon phase was detected by μ-RS, the organization of carbon into tubes is assumed to occur as the liquid Si phase evaporates. Nanotube nucleation begins when the Si vapor pressure in the gap falls below the vapor pressure above the melt droplet surface.

The observed microstructures therefore form according to the following scheme. First, Si microdroplets form and become „pinned“ to the substrate at the steps. A crystalline rim then forms around each droplet, further stabilizing its position. Beneath the droplet, nanotubes nucleate and grow as silicon evaporates, causing increasing carbon supersaturation in the shrinking droplet volume.

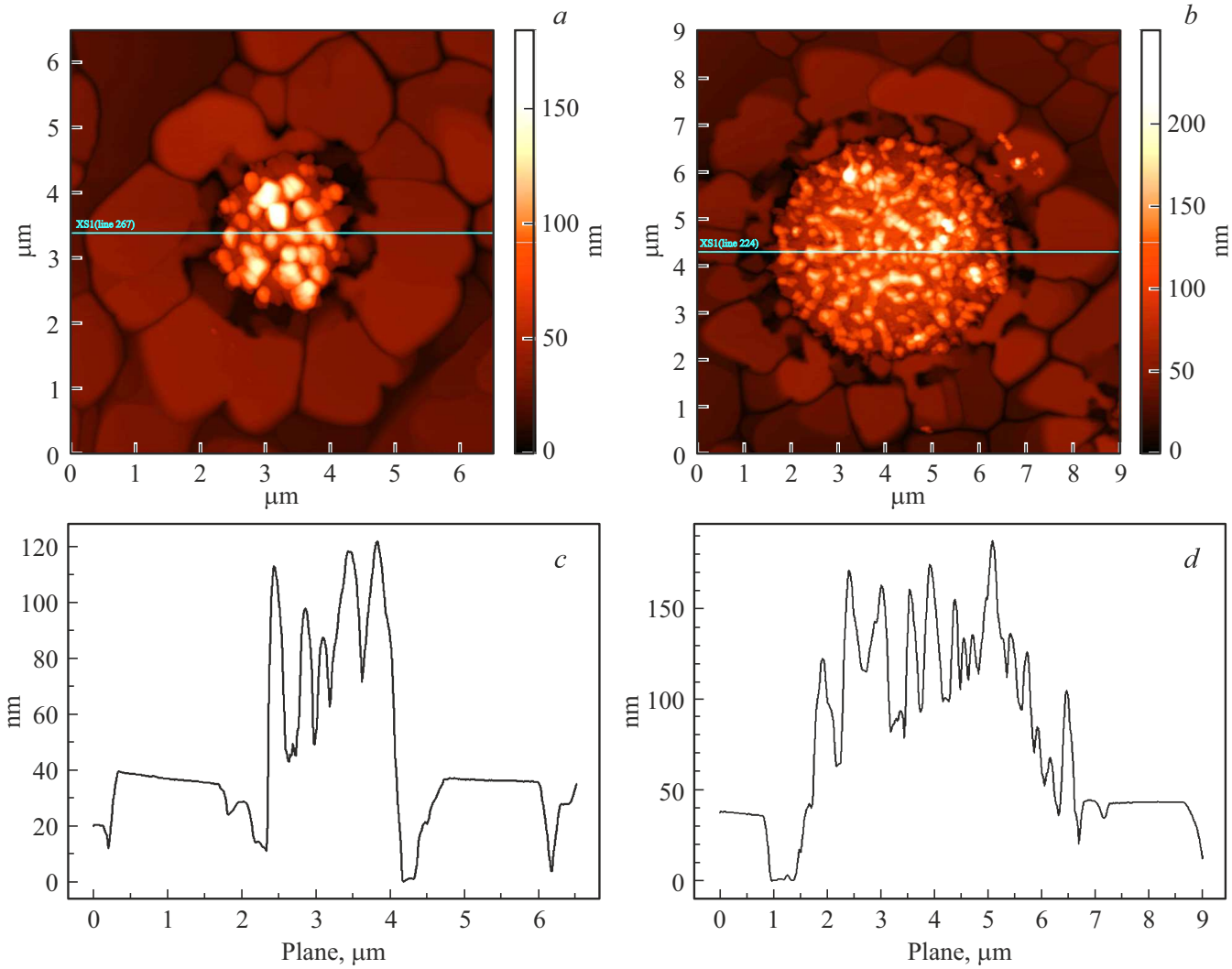


Figure 2. SPM topography (a, b) and corresponding surface profiles (c, d) of differently sized microstructures on a 4*H*-SiC wafer.

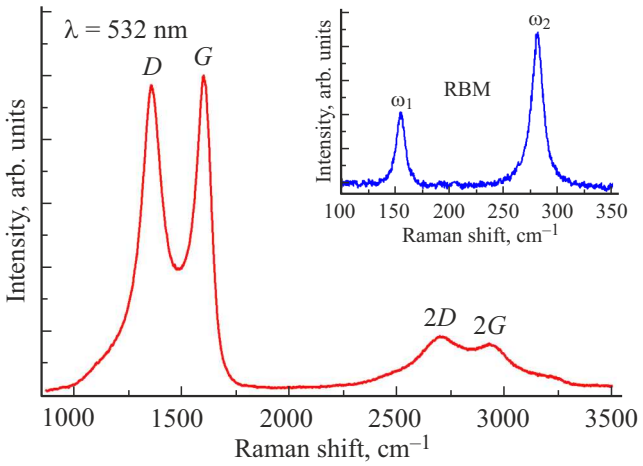


Figure 3. μ-RS spectrum measured in the region of a bundle of vertical substructures. The 4*H*-SiC substrate spectrum has been subtracted for clarity. The inset shows the low-frequency region containing the RBMs.

4. Conclusion

According to the proposed mechanism, SWCNTs form under double spatial confinement imposed by the micrometer-scale melt droplet volume and the submicron gap of the SiC sandwich structure. Nanotube formation within Si melt droplets resembles the conventional VLS mechanism but has a distinctive feature: the melt serves as a medium for CNT self-assembly without metallic catalysts. This enables the production of high-purity SWCNTs integrated with a semiconductor SiC substrate. These findings advance understanding of nanomaterial self-organization in the Si–SiC system.

Funding

This research was supported under the state assignments of the Ministry of Science and Higher Education to the Ioffe Institute (FFUG-2024-0013 and FFUG-2024-0018).

Conflict of interest

The authors declare that they have no conflict of interest.

References

[1] J.H. Lin, C.S. Chen, H.L. Ma, C.W. Chang, C.Y. Hsu, H.W. Chen. Carbon, **46** (12), 1619 (2008). DOI: 10.1016/j.carbon.2008.06.050
[2] B. Liu, W. Ren, L. Gao, S. Li, S. Pei, C. Liu, C. Jiang, H. Cheng. J. Am. Chem. Soc., **131** (6), 2082 (2009). DOI: 10.1021/ja8093907
[3] S. Huang, Q. Cai, J. Chen, Y. Qian, L. Zhang. Am. Chem. Soc., **131** (6), 2094 (2009). DOI: 10.1021/ja809635s
[4] V. Derycke, R. Martel, M. Radosvljevic, F.M. Ross, Ph. Avouris. Nano Lett., **2** (10), 1043 (2002). DOI: 10.1021/nl0256309
[5] P.X. Hou, C. Liu, H.M. Cheng. Carbon, **46** (15), 2003 (2008). DOI: 10.1016/j.carbon.2008.09.009
[6] A.F. Ismail, P.S. Goh, J.C. Tee, S.M. Sanip, M. Aziz. Nano, **3** (3), 127 (2008). DOI: 10.1142/S1793292008000927
[7] J.H. Swisher, L. Jibril, S.H. Petrosko, C.A. Mirkin. Nature Rev. Mater., **7** (6), 428 (2022). DOI: 10.1038/s41578-021-00402-z
[8] M.S. Dresselhaus, G. Dresselhaus, R. Saito, A. Jorio. Phys. Rep., **409** (2), 47 (2005). DOI: 10.1016/j.physrep.2004.10.006
[9] A. Jaud, L. Auvray, A. Kahouli, T. Abi-Tannous, S. Linas, G. Ferro, C. Brylinski. J. Cryst. Growth, **467**, 18 (2017). DOI: 10.1016/j.jcrysgro.2017.03.018
[10] M.G. Mynbaeva, S.P. Lebedev, A.V. Myasoedov, S.Yu. Priobrazhenskii, D.G. Amelchuk. Fiz. Tekh. Poluprovodn., **58** (9), 501 (2024). DOI: 10.61011/FTP.2024.09.59311.6423A (In Russian).